



Cite this: DOI: 10.1039/d0nj00038h

# Detection of hydrogen peroxide using dioxazaborocanes: elucidation of the sensing mechanism at the molecular level by NMR and XPS measurements†

 Thomas Caron,<sup>a</sup> Pascal Palmas,<sup>a</sup> Céline Frénois,<sup>a</sup> Christophe Méthivier,<sup>b</sup> Eric Pasquinet,<sup>\*a</sup> Claire-Marie Pradier,<sup>id b</sup> Françoise Serein-Spirau,<sup>c</sup> Lionel Hairault<sup>a</sup> and Pierre Montméat<sup>id a</sup>

A fluorescent dioxazaborocane was synthesised and characterized, in order to study its turn-off sensing process for hydrogen peroxide detection. The exposure of the dioxazaborocane to diluted vapours of H<sub>2</sub>O<sub>2</sub> led to a strong non reversible quenching of the fluorescence. Both NMR and XPS analyses were carried out before and after exposure of dioxazaborocane to H<sub>2</sub>O<sub>2</sub> vapours. They unequivocally show that the boron atom is oxidised in the film with cleavage of the N–B dative bond. Identification of products such as phenol and boric acid by NMR, supported by consistent XPS data, enabled the whole reaction sequence that explains the fluorescence quenching of dioxazaborocane upon H<sub>2</sub>O<sub>2</sub> exposure to be described accurately. Direct hydrolysis of dioxazaborocane to diol, without oxidation, was only marginally observed.

 Received 3rd January 2020,  
 Accepted 20th February 2020

DOI: 10.1039/d0nj00038h

[rsc.li/njc](http://rsc.li/njc)

## Introduction

The reliable and sensitive detection of hidden explosives in luggage, cars, or aircraft is currently a major issue for law enforcement agencies facing the continuous threat of sudden terrorist attacks. In this context, the detection of peroxide-based explosives (PBEs) in particular triacetone triperoxide (TATP) has now evolved as a crucial need. Hydrogen peroxide (HP), as both a precursor and a decomposition product of such explosives,<sup>1,2</sup> is also an important target. As a matter of fact, detection of HP after UV exposure may constitute a useful indirect sensing method for PBEs.

Among the various strategies that have been described<sup>3,4</sup> for PBE and HP vapour sensing, numerous studies concern solid state gas sensors.<sup>5–32</sup>

In particular, Table 1 summarises the major detection methods and their limit of detection.

They, in particular, include optical and fluorimetric methods, that have drawn increasing attention in recent years due to fast

response, excellent sensitivity (pptv range for<sup>15,16</sup>) and opportunity to be integrated into portable devices.

Our group has already disclosed films of dioxazaborocane 2 as efficient sensors for this purpose.<sup>33</sup> The detection concept that was conceived for 2 took advantage of two different properties. (i) Boron compounds are known to react with hydrogen peroxides through an oxidation process.<sup>34</sup> In solution, this reaction is readily used for alcohol and phenol synthesis, but it is believed that the process may also occur at the solid/gas interface, and (ii) the presence of a nitrogen atom in the side chain usually quenches the anthracene ring fluorescence *via* photoinduced electron transfer (PET).<sup>35</sup>

In 2, the lone pair of the nitrogen atom is involved in the N–B bond and does not interact with the anthracene chromophore, thus resulting in a high fluorescence of the compound. This has been shown in studies dedicated to boronic acid detection in solution through a fluorescence turn-on process, in which the formation of compound 2 was postulated as a complex in solution, though it was not isolated or characterised.<sup>36</sup>

We thought that, using a somewhat reverse turn-off process, upon hydrogen peroxide vapour exposure, a deboronation reaction would release the N lone electron pair so that the anthracene fluorescence would be quenched (Fig. 1).

In this work, we report the synthesis and characterisation of 2, as well as our efforts to obtain the most accurate picture of the chemical reactions that result in its excellent hydrogen peroxide sensing properties in the solid state. Understanding what really occurs at the solid/gas interface is complicated due to technical

<sup>a</sup> CEA-DAM Le Ripault BP 16, F-37260 Monts, France.

E-mail: eric.pasquinet@cea.fr; Fax: +33 247345142

<sup>b</sup> Sorbonne Univ., CNRS, LRS, UMR 7197, LRC n° 1 CEA-UPMC-CNRS, 4 Pl Jussieu, Case Courrier 178, F-75005 Paris, France

<sup>c</sup> Institut Charles Gerhardt, UMR CNRS 5253, Equipe AM2N, Ecole Nationale Supérieure de Chimie de Montpellier, 8, Rue de l'Ecole Normale, 34296 Montpellier Cedex 05, France

† Electronic supplementary information (ESI) available. See DOI: 10.1039/d0nj00038h

Table 1 Detection of peroxide vapours with solid state gas sensors

Ref.	Detection method	Sensitive compound	Limit of detection for HP
5	Optical waveguide	Organic core structure	40 ppbv
10	Fluorescence quenching	EuVO <sub>4</sub>	100 ppbv
12	Fluorescence turn-on	Boronate based polymer	3 ppbv
14	Colorimetric	TiO <sub>2</sub>	200 pptv
15	Fluorescence quenching	Multi-formyl phenols	0.1 pptv
16	Fluorescence quenching	Dioxaborolane	4 pptv
17	Fluorescence turn-on	Dioxaborolane	7 ppbv
18	Colorimetric	Dioxaborolane	2.9 ppbv
19	Fluorescence quenching	Pyrenyl borate	TATP: 0.5 ppmv
20	Fluorescence quenching	Borate ester polymer	1.6 ppbv
22	Impedance spectroscopy	ZnO	100 ppmv
23	Fluorescence turn-on	Boronate quinoline chromophore	150 pptv
24	Fluorescence quenching	Polymer-titanium complex	200 pptv
25	Calorimetry	MnO <sub>2</sub>	2% v
28	Transistor	Phthalocyanines	0.64 ppbv
29	Resistivity	Single-walled carbon nanotubes	25 ppmv

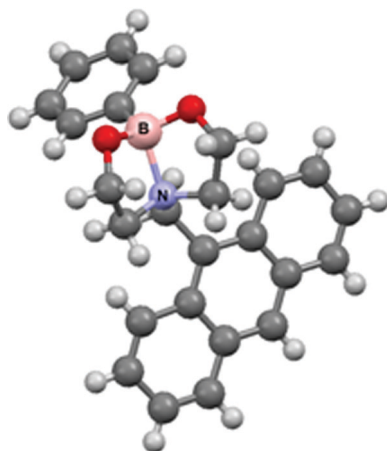


Fig. 1 Molecular structure of dioxazaborocane 2.

issues, including the small amount of molecules that are involved at the film surface. That is why indirect proofs of concepts have been used in related studies, such as IR<sup>7</sup> or UV spectroscopy<sup>20,21</sup> after reaction in solution. Electrochemistry<sup>37</sup> can also be applied in case of the detection of HP with boronate in liquid media. Direct attempts to address the deboronation reaction on borate-ester-based sensing materials have been reported in only very few papers, using IR<sup>21</sup> and absorption spectroscopy.<sup>17,18</sup> Herein, we focused on such direct approaches and exclusively studied solid/gas reactions, monitored by XPS and NMR analyses.

This allowed us not only to evidence the deboronation process on dioxazaborocane 2, but also to unequivocally determine the whole sensing mechanism.

## Experimental section

### Synthesis and characterisation

Dioxazaborocane 2 was obtained as presented in Scheme 2. Diol 1 was obtained as described elsewhere.<sup>38</sup> The chemical reactants were purchased (Aldrich) and used without further purification. Phenylboronic acid (120 mg, 1 mmol) and toluene

(30 mL) were introduced into a Dean–Stark apparatus. The mixture was refluxed for 5 h and then cooled to room temperature before filtration and washing with toluene.

All NMR measurements were performed at 21 °C on a Bruker Avance 400 MHz spectrometer. We used a standard Bruker 5 mm BBFO+ probe for <sup>1</sup>H, <sup>13</sup>C and <sup>11</sup>B experiments. Samples were prepared using quartz tubes, in order to reduce the wide line <sup>11</sup>B contribution of the borosilicate. Despite this, a residual response, probably coming from the probe itself, was observed.

It was suppressed from the spectra afterwards by a simple baseline correction. <sup>1</sup>H and <sup>13</sup>C experiments were calibrated according to the solvent signal used as a secondary internal reference (CDCl<sub>3</sub>: <sup>1</sup>H: 7.27 ppm; <sup>13</sup>C: 77.2 ppm; MeOD <sup>1</sup>H: 3.31 ppm; <sup>13</sup>C: 49.2 ppm in respect with TMS, 0 ppm). For <sup>11</sup>B chemical shifts, the rather sharp signal of phenylboronic acid (C<sub>6</sub>H<sub>5</sub>–B(OH)<sub>2</sub>) solution in ethanol-d<sub>6</sub> (δ = 28.4 ppm)<sup>43</sup> with respect to BF<sub>3</sub>–Et<sub>2</sub>O (δ = 0 ppm) was used as an external secondary reference.

XP spectra were collected on a SPECS GmbH PHOIBOS 100-1D delay line detector photoelectron spectrometer, using a monochromatised Al Kα (1486.6 eV) radiation source with 250 W electron beam power. The samples were analysed under ultra-high vacuum conditions (1 × 10<sup>−8</sup> Pa). After recording a broad range spectrum (pass energy 100 eV), high-resolution spectra were recorded for the B1s, N1s, C1s, O1s core XPS levels (pass energy 20 eV). Spectrum processing was carried out using the Casa XPS software package.

IR spectra were recorded on an ATR PerkinElmer 100 spectrophotometer.

Melting points were measured with a TA Instruments Q100 DSC (heating rate: 10 °C min<sup>−1</sup>).

High-resolution mass spectra (HRMS) were obtained using impact ionisation (EI) with PFTBA as internal standard. Spectra were recorded on the Accu-TOF GC JEOL.

The X-ray data collection of the single crystals was performed at 173 K on an Oxford-Diffraction GEMINI-S single crystal diffractometer, using graphite-monochromatised Mo Kα radiation (λ = 0.71073 Å).

The three-dimensional structures were solved by *ab initio* methods, such as those implemented in the charge-flipping

algorithm.<sup>39</sup> The structural refinements were performed with the CRYSTALS package<sup>40</sup> on Fobs using reflections with  $I > 2\sigma(I)$ . CCDC 1543590 contains the supplementary crystallographic data for this paper.†

### Film deposition

Dioxazaborocane **2** was deposited on the entire surface of a glass substrate (microscope slide 75 mm × 25 mm × 1 mm) by spin coating (Braive Instrument spin coater – 600 rpm for 60 s) from a chloroform solution (5 mg mL<sup>-1</sup>). The absorption intensity at 373 nm, measured using a PerkinElmer Lambda 35 spectrometer, was between 0.2 and 0.4.

### Detection tests

Chemical gas detections were performed on water and HP (30%) using a fluorescent laboratory prototype. A more detailed description of the instrument was given previously.<sup>41</sup> The hydrogen peroxide concentration was evaluated by a commercial detector (Polytron<sup>®</sup>7000-Dräger): 50 ppmv. Dioxazaborocane film has been used as sensing materials on the microscope slide acting as transducer and substrate. The prototype line was connected to the generation cell; equilibrated at the vapour pressure of compound. The sensor response was expressed as a percentage of fluorescence inhibition.

### Sensing mechanism study

For the sensing mechanism comprehension, a specific setup was used to generate HP vapours and exposed powder of dioxazaborocane. A dynamic method based on evaporation was chosen to produce HP vapours at controlled and constant concentrations, over a long period of time (19 h, 48 h). Fine powder of **2** (130 mg) was thus exposed at 100 ppmv of HP. For NMR characterisation after exposure, 10 mg of **2** were sampled and diluted in 4 mL of CDCl<sub>3</sub> or MeOD. All of the experiments were carried out at between 15 °C and 23 °C.

## Results and discussion

### Synthesis and characterisation of dioxazaborocane **2**

Dioxazaborocane **2** was obtained in a 64% yield as fluorescent crystals (250 mg).

The product was fully characterised and suitable crystals for XRD studies were obtained after recrystallisation in toluene. Complete data are available in ESI,† S1 and S2.

The molecular structure is shown in Fig. 1.

The crystallographic structure confirms the tetrahedral geometry of the boron atom and the presence of a dative B–N bond. The B–N and B–O bond lengths lie within the ranges of 1.767–1.745 and 1.431–1.443 Å, respectively (the asymmetric unit contains 2 molecules). These values are in agreement with those reported for already known *N*-substituted dioxazaborocanes.<sup>42</sup> The B–N bond is, however, somewhat lengthier than for the other related compounds (typically 1.70–1.72 Å for the latter). The B–N bond is even shorter for *N*-H dioxazaborocanes.<sup>43</sup> Since it has been shown that substitution on the B atom was of little

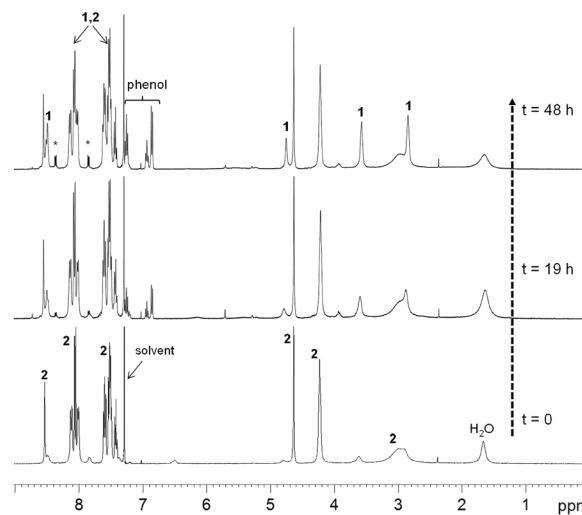


Fig. 2 Evolution of the <sup>1</sup>H NMR spectrum of **2** in CDCl<sub>3</sub> as a function of time of exposure to HP. Small peaks indicated by a star correspond to product degradation not directly due to HP.

influence,<sup>42b</sup> it seems that the B–N bond length is more sensitive to substitution on the N atom.

NMR characterisation of **2** was performed using CDCl<sub>3</sub> as solvent. The <sup>1</sup>H spectrum is displayed in Fig. 2 and partial assignment is given therein. NMR data of **2** in the same solvent had been already reported,<sup>36c</sup> but the <sup>1</sup>H information on methylene moieties was missing, seemingly due to large broadening. The same broadening effect was observed here, but the peaks were readily detectable. Hence, chemical shifts [ $d = 4.62$  (s, 2 H), 4.21 (s, 4 H), 2.96 (s, 4 H) ppm] were measured for methylene protons and [ $d = 8.51$  (s, 1 H), 8.02 (m, 6 H), 7.50 (m, 7 H) ppm] in the aromatic region, some of which were significantly different from those of diol **1**. In compensation, <sup>13</sup>C chemical shifts of methylene carbons were given<sup>36c</sup> and agree well with present values  $d = 63.0, 56.4, 51.9$  ppm (spectrum not shown). Turning to the <sup>11</sup>B spectrum, a single line was observed at 14 ppm. Such a chemical shift is characteristic of a sp<sup>3</sup> hybridisation and thus with the formation of a N → B dative bond, in agreement with XRD data. The slight difference with the published value of 15.9 ppm certainly results from a different referencing, as the reported phenylboronic acid chemical shift was 32.27 ppm instead of 29.6 ppm in our case. Moreover, chemical shift values lying within the same range [12–13 ppm] were also reported for similar systems.<sup>42b–44</sup>

### Hydrogen peroxide sensing

Fig. 3 presents the fluorescence intensity shift of a thin film of **2** upon exposure to water vapours for 10 minutes, then to hydrogen peroxide vapours for 10 minutes. While the signal remained almost unchanged in the presence of water (less than 5% fluorescence decrease), 64% of the fluorescence **2** was quenched by HP vapours. This highlighted the potential interest of **2** as a sensing material for HP and peroxide-based explosives. In our test conditions and based on our fluorescent laboratory prototype performances,<sup>41</sup> we can estimate the limit

of detection around 4 ppmv (see ESI† S3 for details). Otherwise, the response of films of **2** was clearly irreversible, suggesting that a chemical reaction occurred between HP and **2**. This would be consistent with the postulated concept and this prompted us to investigate the detection mechanism resulting in the fluorescence quenching of **2** in greater depth.

### Sensing mechanism: NMR and XPS experiments

Our detection turn-off concept was based on the oxidation of the boron atom of the fluorescent compound **2**, which would lead to the non-fluorescent diol **1**. Both NMR and XPS experiments were designed to obtain the most accurate picture of what was happening at the surface of **2** during exposure to hydrogen peroxide vapours. Our aim was not only to prove the oxidation of the boron atom, but also to identify the molecular species that were generated in the whole process.

Similar molecular approaches are very scarce in the literature for the detection of peroxide<sup>19,21</sup>

Fig. 3 displays the <sup>1</sup>H spectrum of **2** after being exposed to HP vapours. There were several modifications in the spectrum, which increased as a function of exposure time. This is one key to the demonstration, as it showed without ambiguity what changes were related to the detection process and not to a possible degradation of the product. First, several peaks grew together as a function of exposure time with chemical shifts close to those originating from **1**, suggesting a quite similar structure. Due to the fact that the lines were broader and originally present in **2** as weak contributions, we initially thought of a possible equilibrium between the bicyclic coordinated tetrahedral boron species with a possible “open” form, bearing an 8-membered ring and lacking the N → B dative bond, as suggested in ref. 43 However, the interpretation of the entire set of NMR observations led us to the conclusion that these growing peaks were due to diol **1**, a weak proportion of which was initially present in **2**, and that they increased with exposure time. This assignment was confirmed by comparison with a second spectrum acquired after addition of a small

amount of pure **1**. An increase in the existing peaks was observed, accompanied by a line broadening and a slight chemical shift displacement. This procedure gives stronger evidence than a simple comparison with a spectrum of the pure compound in the same solvent, because environmental effects on chemical shifts and line width can be different from the real sample. It must be noticed that a separate OH proton signal from **1** at 2.3 ppm was not detected. This is due to an exchange with a water proton in the presence of **2** and phenol (*vide supra*) that leads to a large broadening and collapse at an intermediate chemical shift. Second, the increasing quantity of **1** was accompanied by the appearance and gradual growth of three other multiplets in the aromatic region. These peaks were clearly assigned to free phenol following the same procedure as described above (addition of phenol). Conversely, phenylboronic acid was also added to the sample to demonstrate the absence of this compound in **2** before and after exposure to HP. Additional smaller contributions (marked by a star) were also detected as two symmetrical doublets in the aromatic region. A dramatic increase in their intensity was observed when a <sup>1</sup>H experiment was performed on the same sample a few days later. They were consequently attributed to a “natural” degradation of **2** that occurred at least when dissolved in an organic solvent and, in any case, independent from the HP treatment.

These results were further confirmed by <sup>13</sup>C NMR but, finally, the elucidation of the whole detection mechanism required <sup>11</sup>B NMR measurements and the use of a different solvent.

The <sup>11</sup>B spectrum in CDCl<sub>3</sub> of **2** acquired after exposure to HP still contained only one line at 14 ppm, which was assigned to compound **2** itself (see ESI† S4). Phenylboronic acid was thus missing both in the starting material and after reacting with HP, as this compound gives a rather sharp line at 29.6 ppm. This is in accordance with the <sup>1</sup>H NMR observations. A different situation was seen using MeOD as solvent, in which **2** was completely dissociated into **1** and phenylboronic acid. This was obvious from the <sup>1</sup>H spectrum first, and further confirmed by the observation of a single <sup>11</sup>B signal at 28.4 ppm (Fig. 4). This was also in accordance with the fact that MeOH solutions of **2** were not fluorescent.

Of course, this line was still present after exposure to HP and came from residual **2** that had not reacted. It turned out that such a complete dissociation of **2** made MeOD inappropriate to follow any transformation into **1** occurring during HP exposure. However, a new <sup>11</sup>B component was revealed at 18.8 ppm, whose intensity (relative to phenylboronic acid) increased as a function of time. This chemical shift is compatible with boric acid,<sup>44</sup> a product that was not soluble in CDCl<sub>3</sub>. This assignment was again confirmed by addition of boric acid (also in Fig. 4), thus ruling out other hypotheses (“open” 8-membered ring, intermediate **3**). All of these features were also observed using DMSO as the solvent (not shown).

In the conclusions of the NMR study, it is demonstrated that **2**, upon exposure to HP vapours, produces diol **1**, boric acid and phenol.

XPS experiments were also carried out to get additional information on the chemical processes involved, especially at

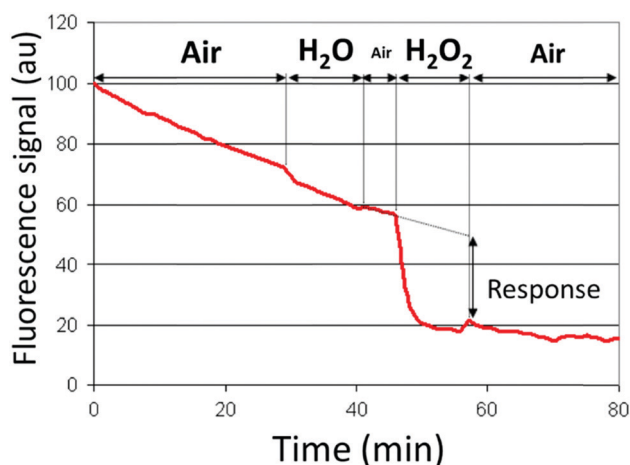


Fig. 3 Fluorescence quenching of a film of **2** upon successive exposures to water and hydrogen peroxide vapours.

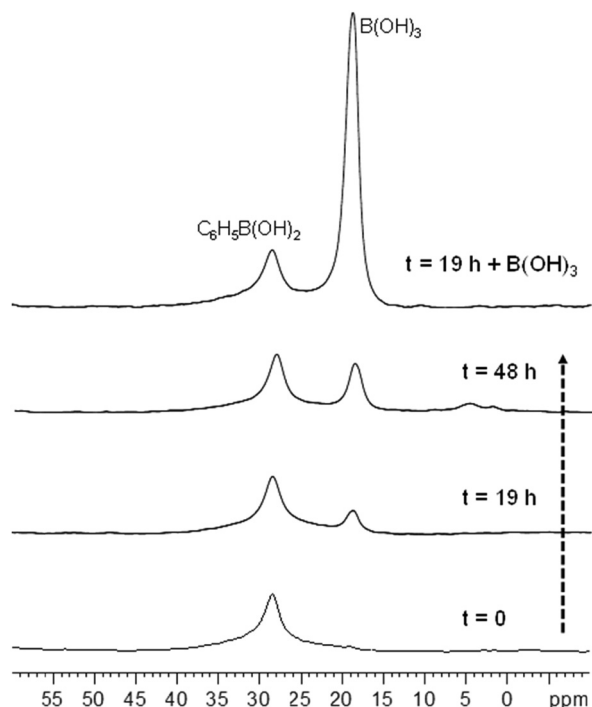


Fig. 4 Evolution of  $^{11}\text{B}$  NMR spectra of **2** in MeOD as a function of exposure to HP vapours. The spectrum at the top was recorded (for assignment purpose) after the addition of a small amount of  $\text{B}(\text{OH})_3$  to the NMR sample ( $t = 19$  h).

the surface. Fig. 5 shows the high-resolution XPS spectra recorded for the N1s and B1s region for dioxazaborocane **2** just synthesised (spectrum a), after having been exposed to  $\text{H}_2\text{O}_2$  for 2 h (spectrum b) and for 48 hours (spectrum c).

The narrow and symmetric peak observed before any exposure and centred at 400.5 eV is in agreement with the chemistry of the nitrogen atom of a dioxazaborocane structure, bound to 3 carbon atoms and one boron atom ( $\text{sp}^3$  hybridisation). In the B 1s region, a peak is observed at 190.5 eV, which is a fingerprint of an electron-rich B atom. This is easily explained by the electron transfer of a doublet from the N atom, thus constituting a bond between the N and the B atom of the molecule (N–B dative bond), as schematised in Scheme 1 (tetrahedral geometry of the boron atom). This is in perfect agreement with the XRD and NMR data.

After exposure to hydrogen peroxide vapours, XPS spectra undergo significant changes. After 2 h, the N1s peak of dioxazaborocane **2** is much broader, with two new contributions in addition to that at 400.5 eV. The one at higher binding energy (BE), *ca.* 402.2 eV, suggests a positive charge on the N atom, while that at lower BE, *ca.* 398.8 eV, bears testimony to an additional negative charge on the nitrogen atom. After a 48 h exposure, the N1s peak is dominated by the contribution at 402.2 eV.

Simultaneously, the B1s peak also changes, displaying, after exposure for 2 h, a new contribution at 191.8 eV, which shows a lower negative charge on the boron atom. After 48 h, the pristine contribution at 190.4 eV has almost disappeared to the benefit of

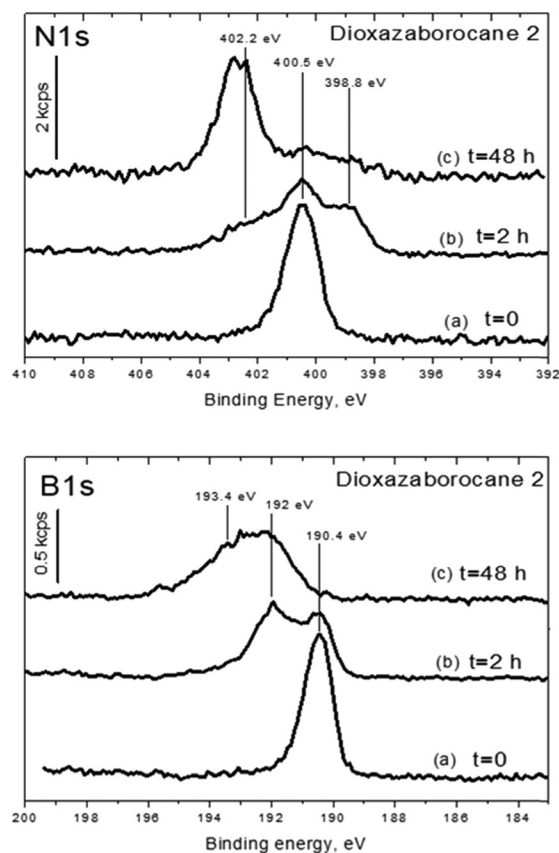
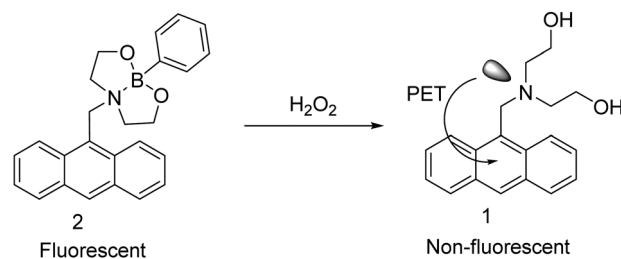
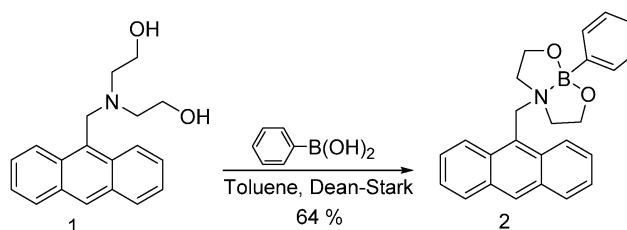


Fig. 5 Evolution of N1s and B1s X-ray photoelectron spectra of **2** as a function of exposure to HP vapours.



Scheme 1 Sensing concept: fluorescence turn-off upon hydrogen peroxide exposure to dioxazaborocane **2**.



Scheme 2 Synthesis of dioxazaborocane **2**.

peaks at 192 and 193.4 eV. The latter contribution is compatible with the formation of boric acid,  $\text{B}(\text{OH})_3$ ,<sup>45</sup> while the former is indicative of an intermediate species. Phenylboronic acid, as a

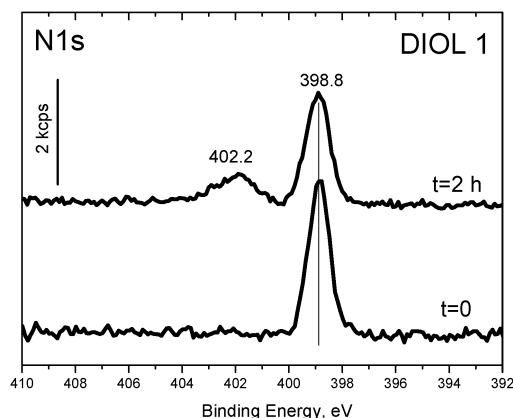


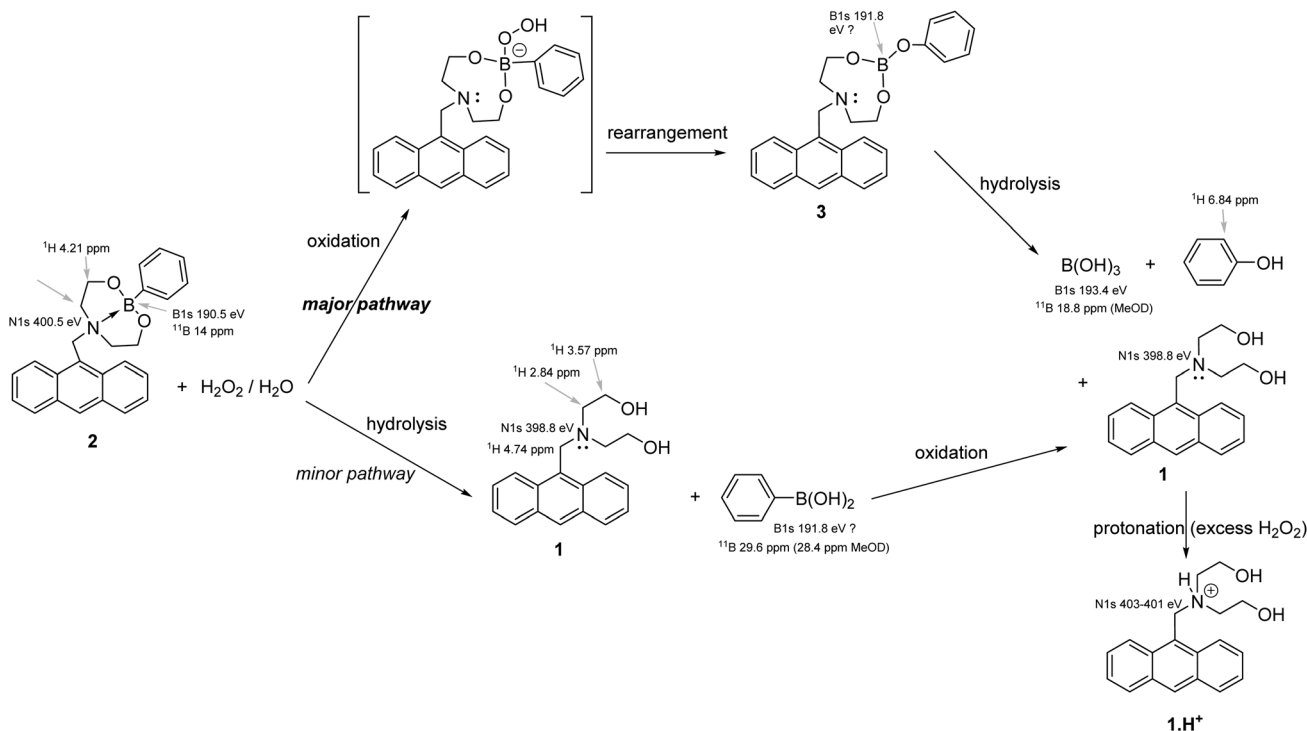
Fig. 6 Evolution of N1s X-ray photoelectron spectra of **1** before and after exposure to HP vapours.

hydrolysis product, could be a possibility B1s was reported to be at 192 eV,<sup>46</sup> but a control experiment showed that hydrolysis only marginally occurred when **2** was subjected to water vapours (recording of XPS spectra before and after exposure for 2 h indicated only around 10% formation of phenylboronic acid. This is consistent with the very small response of films of **2** upon exposure to water, see Fig. 2). Moreover, phenylboronic acid was never observed in the NMR experiments. The rearrangement product **3** would also be expected to give a peak around 192 eV, however, we were unable either to isolate this product for XPS identification, or to confirm its formation by <sup>11</sup>B NMR.

In order to explain the changes in the electronic states of the N atom, diol **1** was in turn analysed by XPS in its pristine form and after 2 hours of exposure to hydrogen peroxide. The N1s spectra obtained are presented in Fig. 6, showing a very interesting evolution. The narrow N 1s peak observed for the diol is indeed characteristic of a nitrogen atom bound to three carbon atoms, and still bearing an electron doublet, while, after exposure to H<sub>2</sub>O<sub>2</sub>, a new contribution appears at 402.2 eV, typical of an ammonium type nitrogen (see Scheme 3). The latter contribution is at exactly the same binding energy as that of dioxazaborocane **2** after 48 h under H<sub>2</sub>O<sub>2</sub>. These data are strong suggestions that exposure of **2** to H<sub>2</sub>O<sub>2</sub> induces a strong alteration of the chemical bonds on a fraction of the compound, in particular a breaking of the N–B dative bond, together with an oxidation (in the electronic sense) of the nitrogen atom. A longer exposure to H<sub>2</sub>O<sub>2</sub> leads to the protonation of the N atom due to the acidic nature of hydrogen peroxide.

To summarise the situation, XPS data are in strong agreement with a substantial chemical reactivity of dioxazaborocane **2** upon exposure to H<sub>2</sub>O<sub>2</sub>. It results into a mixture of diol **1**, its protonated form **1.H**<sup>+</sup>, boric acid, another boron-containing compound (maybe intermediate **3**) and traces of unreacted dioxazaborocane **2**.

It is noteworthy that XPS data, focusing only on surface layers (5–10 nm), were found both consistent and complementary with NMR data, which probe the entire samples. These XPS and NMR data, as well as detection results, strongly support the mechanism depicted in Scheme 3. Upon exposure to vapours of



Scheme 3 Chemical transformations of dioxazaborocane **2** upon exposure to vapours of aqueous hydrogen peroxide, as supported by selected NMR and XPS assignments (all chemical shifts in CDCl<sub>3</sub> unless otherwise stated).

aqueous hydrogen peroxide, fluorescent dioxazaborocane **2** is mainly oxidised to the expected intermediate **3** through a commonly accepted mechanism,<sup>34</sup> followed by hydrolysis to get a mixture of non-fluorescent diol **1**, boric acid and phenol. Part of **1** is protonated with excess HP to  $1.H^+$ . Another pathway, leading to the same ultimate products, also occurs but to a lesser extent. In this case, hydrolysis is the first reaction, thus producing diol **1** and phenylboronic acid. The latter is then oxidised<sup>47</sup> and hydrolysed to boric acid and phenol.

## Conclusions

In the context of detection of hidden peroxide explosives, a dioxazaborocane compound as an efficient hydrogen peroxide (HP) sensing material was synthesised and characterised. When exposed to diluted vapours of HP, the fluorescence of a thin film of this material strongly decreased. NMR and XPS studies on dioxazaborocane after exposure to HP vapours showed that the N–B dative bond is cleaved with oxidation of the boron atom. Identification of phenol and boric acid as end products allowed us to accurately describe the whole reaction sequence that explains the fluorescence quenching of dioxazaborocane upon HP exposure.

## Conflicts of interest

There are no conflicts to declare.

## Acknowledgements

Arie van der Lee is acknowledged for XRD experiments.

## References

- R. Shulte-Ladbeck, P. Kolla and U. Karst, *Analyst*, 2002, **127**, 1152–1154.
- R. Shulte-Ladbeck, P. Kolla and U. Karst, *Anal. Bioanal. Chem.*, 2006, **386**, 559–565.
- Counterterrorist Detection Techniques of Explosives*, ed. J. Yinon, Elsevier, Amsterdam, 2009.
- R. Burks and D. Hage, *Anal. Bioanal. Chem.*, 2009, **395**, 301–313.
- J. Y. Zheng, Y. Yan, X. Wang, W. Shi, H. Ma, Y. S. Zhao and J. Yao, *Adv. Mater.*, 2012, **24**, OP194–OP199.
- H. Lin and K. S. Suslick, *J. Am. Chem. Soc.*, 2010, **132**, 15519–15521.
- M. Xu, B. R. Bunes and L. Zang, *ACS Appl. Mater. Interfaces*, 2011, **3**, 642–647.
- A. Mills, P. Grosshans and E. Snadden, *Sens. Actuators, B*, 2009, **136**, 458–463.
- M. Schäferling, D. Gröge and S. Schrem, *Microchim. Acta*, 2011, **174**, 1–18.
- C. Ambard, N. Duée, F. Pereira, D. Portehault, C. Méthivier, C.-M. Pradier and C. Sanchez, *J. Sol-Gel Sci. Technol.*, 2016, **79**, 381–388.
- A. Fang, PhD thesis, University of California, USA, 2004.
- J. Sanchez and W. Trogler, *J. Mater. Chem.*, 2008, **18**, 5134–5141.
- (a) M. L. Grone, *US Pat.*, McAfee & Taft, 2010/0144050, 2010; (b) R. Deans, A. Rose, K. Bardon, L. Hancock and T. Swager, WO 2008/073173, Nomadics Inc., 2008; (c) R. Deans, A. Rose, B. O'Dell and M. La Grone, WO 2008/121124, Nomadics Inc., 2008.
- P. Marks, B. Radaram, M. Levine and I. A. Levitsky, *Chem. Commun.*, 2015, **51**, 7061–7064.
- W. Xu, Y. Fu, Y. Gao, J. Yao, T. Fan, D. Zhu, Q. He, H. Cao and J. Cheng, *Chem. Commun.*, 2015, **51**, 10868–10870.
- Y. Fu, J. Yao, W. Xu, T. Fan, Z. Jiao, Q. He, D. Zhu, H. Cao and J. Cheng, *Anal. Chem.*, 2016, **88**, 5507–5512.
- M. Xu, J.-M. Han, C. Wang, X. Yang, J. Pei and L. Zang, *ACS Appl. Mater. Interfaces*, 2014, **6**, 8708–8714.
- M. Xu, J.-M. Han, Y. Zhang, X. Yang and L. Zang, *Chem. Commun.*, 2013, **49**, 11779.
- C. He, D. Zhu, Q. He, L. Shi, Y. Fu, D. Wen, H. Cao and J. Cheng, *Chem. Commun.*, 2012, **48**, 5739–5741.
- L. Chen, Y. Gao, Y. Fu, D. Zhu, Q. He, H. Cao and J. Cheng, *RSC Adv.*, 2015, **5**, 29624–29630.
- L. Zang, J. Han and M. Xu, *US Pat.*, 2014/0193923 A1, Univ. Utah Research Foundation, 2014.
- G. H. Shahkhatuni, V. M. Aroutiounian, V. M. Arakelyan, M. S. Aleksanyaa and G. E. Shahnazaryan, *J. Contemp. Phys.*, 2019, **54(2)**, 188–195.
- B. P. Garrefffi, M. Guo, N. Tokranova, N. C. Cady, J. Castracane and I. A. Levitsky, *Sens. Actuators, B*, 2018, **276**, 466–471.
- P. Marks, B. Radaram, M. Levine and I. A. Levitsky, *Chem. Commun.*, 2015, **51**, 7061.
- J. Oberländer, P. Kirchner, H.-G. Boyen and M. J. Schöning, *Phys. Status Solidi A*, 2014, **211(6)**, 1372–1376.
- T. S. Sheriff, S. Miah and K. L. Kuok, *RSC Adv.*, 2014, **4**, 35116.
- J. Hennemann, C.-D. Kohl, S. Reisert, P. Kirchner and M. J. Schöning, *Phys. Status Solidi A*, 2013, **210(5)**, 859–863.
- J. E. Royer, E. D. Kappe, C. Zhang, D. T. Martin, W. C. Trogler and A. C. Kummel, *J. Phys. Chem. C*, 2012, **116**, 24566–24572.
- Y. Lu, M. Meyyappan and J. Li, *Small*, 2011, **7(12)**, 1714–1718.
- M. Xu, B. R. Bunes and L. Zang, *ACS Appl. Mater. Interfaces*, 2011, **3**, 642–647.
- F. I. Bohrer, C. N. Colesniuc, J. Park, I. K. Schuller, A. C. Kummel and W. C. Trogler, *J. Am. Chem. Soc.*, 2008, **130**, 3712–3713.
- J. C. Sanchez and W. C. Trogler, *J. Mater. Chem.*, 2008, **18**, 5134–5141.
- T. Caron, M. Bouhadid, E. Pasquinet, P. Montméat and F. Serein-Spirau, *CEA*, WO 2012/052399, 2012.
- M. B. Smith and J. March, *March's advanced organic chemistry*, Wiley, Hoboken, 6th edn, 2007, pp. 1779–1780.
- (a) R. Bissell, E. Calle, A. Prasanna de Silva, S. de Silva, N. Gunaratne, J. L. Habib-Jiwan, A. Peiris, D. Rupasinghe,

- S. Samarasinghe, S. Sandanayake and J. P. Soumillon, *J. Chem. Soc., Perkin Trans. 2*, 1992, 1559–1563; (b) F. Pina, A. Bernardo and E. Garcia-Espana, *Eur. J. Inorg. Chem.*, 2000, 2143–2157.
- 36 (a) W. Wang, G. Springsteen, S. Gao and B. Wang, *Chem. Commun.*, 2000, 1283–1284; (b) G. Springsteen, E. Ballard, S. Gao, W. Wang and B. Wang, *Bioorg. Chem.*, 2001, **29**, 259–270; (c) S. Arimori and T. James, *Tetrahedron Lett.*, 2002, **43**, 507–509.
- 37 L. Hu, S. Han, Z. Liu, S. Parveen, Y. Yuan and G. Xu, *Electrochem. Commun.*, 2011, **13**, 1536–1538.
- 38 W. Wang, G. Springsteen, S. Gao and B. Wang, *Chem. Commun.*, 2000, 1283–1284.
- 39 L. Palatinus and C. Chapuis, *J. Appl. Crystallogr.*, 2007, **40**, 786–790.
- 40 P. W. Betteridge, J. R. Carruthers, R. I. Cooper, K. Prout and D. J. Watkin, *J. Appl. Crystallogr.*, 2003, **36**, 1487.
- 41 (a) E. Schultz, R. Galland, D. Du Bouëtiez, T. Flahaut, A. Planat-Chrétien, F. Lesbre, A. Hoang, H. Volland and F. Perraut, *Biosens. Bioelectron.*, 2008, **23**, 987–994; (b) T. Caron, M. Guillemot, P. Montméat, F. Veignal, F. Perraut, P. Prené and F. Serein-Spirau, *Talanta*, 2010, **81**, 543–548.
- 42 (a) J. Sopkova de Oliveira Santos, A. Bouillon, J.-C. Lancelot and S. Rault, *Acta Crystallogr.*, 2004, **C60**, o582–o584; (b) E. Kh. Lermontova, M. M. Huang, S. S. Karlov, M. V. Zabalov, A. V. Churakov, B. Neumüller and G. S. Zaitseva, *Russ. Chem. Bull., Int. Ed.*, 2008, **57**, 1920–1930; (c) N. Farfan, T. Mancilla, D. Castillo, G. Uribe, P. Joseph-Nathan and R. Contreras, *J. Organomet. Chem.*, 1990, **381**, 1–13.
- 43 H. Bonin, T. Delacroix and E. Gras, *Org. Biomol. Chem.*, 2011, **9**, 4714–4724.
- 44 H. Nöth and B. Wrackmeyer, in *Nuclear Magnetic Resonance spectroscopy of Boron Compounds*, ed. P. Diehl, E. Fluck and R. Kosfeld, Springer-Verlag, Berlin Heidelberg New York, 1978, pp. 136, 140, 301.
- 45 D. N. Hendrickson, J. M. Hollander and W. L. Jolly, *Inorg. Chem.*, 1970, **9**, 612.
- 46 B. Fabre and F. Hauquier, *Langmuir*, 2017, **33**, 2693.
- 47 R. B. Wagh and J. M. Nagarkar, *Tetrahedron Lett.*, 2017, **58**, 4572–4575.